

# Use of Experimental Separation Limits in the Theoretical Design of V/STOL Inlets

Michael A. Boles\*

*Indiana Institute of Technology, Fort Wayne, Ind.*

and

Norbert O. Stockman†

*NASA Lewis Research Center, Cleveland, Ohio*

Experimental data from several model inlets have been used to generate two parameters which are related to the limit of operation for inlet flow separation. One parameter, called the diffusion ratio, is the ratio of the peak velocity on the inlet surface to the velocity at the diffuser exit and is related to the boundary-layer separation at low throat Mach numbers. The other parameter, the peak Mach number on the inlet surface, is related to the separation at high throat Mach numbers. These parameters are easily calculated from potential flow solutions and thus can be used as a design tool in screening proposed inlet geometries. Any of the geometric design variables can be analyzed by this technique; but, this paper is restricted to the consideration of the internal lip contraction ratio. An illustrative example of an application to an inlet design study for a tilt-nacelle VTOL airplane is presented. The study will show what value of contraction ratio is required to meet the operating requirements yet allow the inlet to remain free of separation as indicated by the two separation parameters.

## Nomenclature

$A$	= area
$a$	= major axis of internal lip (Fig. 1)
$b$	= minor axis of internal lip (Fig. 1)
$D$	= diameter
$L$	= length (Fig. 1)
$M$	= Mach number
$P_s$	= static pressure
$P_T$	= total pressure
$S$	= local surface distance from inlet highlight (Fig. 1)
$S_{ref}$	= surface distance from inlet highlight to diffuser exit (Fig. 1)
$V$	= velocity
$\bar{x}$	= external forebody length (Fig. 1)
$x$	= axial distance from inlet highlight
$\bar{y}$	= external forebody thickness (Fig. 1)
$y$	= radial distance from inlet highlight
$\alpha$	= incidence angle of inlet, angle between freestream velocity and inlet axis (Fig. 1)

## Subscripts

$c$	= centerbody
$d$	= diffuser
$e$	= exit
$h$	= highlight
max	= maximum
$t$	= throat
$0$	= freestream

## Introduction

**P**ROPOSED V/STOL aircraft for both civilian and military applications require propulsion system inlets to operate efficiently over wide ranges of freestream velocity, incidence angle, and inlet throat Mach number (mass flow rate). For example, flight conditions during a vertical takeoff

Presented as Paper 77-878 at the AIAA/SAE 13th Propulsion Conference, Orlando, Fla., July 11-13, 1977; submitted Nov. 28, 1977; revision received July 28, 1978. Copyright © American Institute of Aeronautics and Astronautics, Inc., 1977. All rights reserved.

Index categories: Aerodynamics; Boundary-Layer Stability and Transition.

\*Head, Division of Engineering and Associate Professor of Mechanical Engineering.

†Aerospace Engineer, Wind Tunnel & Flight Division. Member AIAA.

and landing may result in very large inlet incidence angles (up to 120 deg). A major concern for the designer in maintaining efficient operation at these severe conditions is possible inlet internal flow separation. Separation-free internal flow is desired to minimize fan blade stress and prevent the possibility of compressor stall. These flow requirements are quite severe for a fixed-geometry inlet; thus, considerable development work must be accomplished to provide separation-free operation.

The effects of geometry and flow conditions on V/STOL inlet performance have been reported in Refs. 1-7. These studies include experimental performance results for short-haul aircraft engine inlets<sup>1-4</sup> and theoretical studies.<sup>3-7</sup>

This paper presents experimental data from several model STOL inlet tests for two parameters that may be expected to influence flow separation and thus inlet performance. One parameter called the diffusion ratio<sup>8</sup> is the ratio of the peak velocity on the inlet surface to the velocity at the diffuser exit and is related to the boundary-layer separation at low throat Mach numbers. The other parameter, the peak Mach number on the inlet surface, is related to the separation at high throat Mach numbers. By identifying these parameters as measures of the likelihood of flow separation, an assessment can be made of inlet geometric design parameters for separation-free operation.

These STOL experimental results will be applied to potential flow results for a set of typical VTOL engine tilt-nacelle geometries. Specific geometries may then be identified for regions of separation-free operation and for further theoretical and/or experimental study.

## Separation Limits

Engine inlets required to operate under the flight conditions of VTOL aircraft experience increasing inlet surface velocities on the inlet internal lip for increasing incidence angle and throat Mach number. With these higher surface velocities, greater amounts of deceleration must occur on the inlet surface between the maximum velocity location and the diffuser exit. If the amount of flow deceleration is too great, flow separation may develop.<sup>8</sup> This paper investigates the possibility of using two potential flow parameters, the peak Mach number (on the inlet surface) and the diffusion ratio (ratio of maximum surface velocity to diffuser exit surface

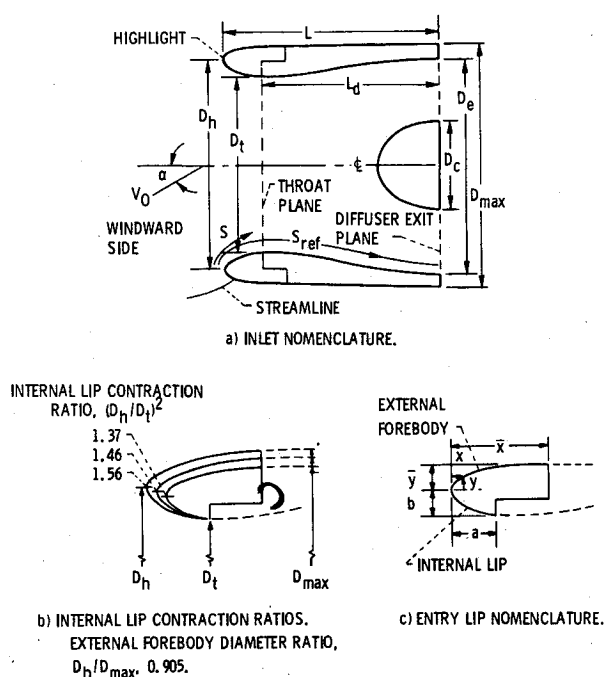


Fig. 1 Inlet nomenclature and range of geometric variables for STOL test inlets.

velocity), to screen VTOL engine inlet geometries for possibility of flow separation at prescribed flow conditions.

To aid in the analysis of a given surface velocity distribution for the possibility of flow separation, Ref. 8 recommends nondimensionalizing the local surface velocity by the maximum velocity (local velocity ratio). Flow conditions resulting in the same dimensionless local velocity ratio distribution over the flow surface have the same flow separation characteristics at the same Reynolds number. When the local velocity ratio goes below a certain value (dependent upon conditions prior to diffusion) separation is indicated.

In the present paper the concept of Ref. 8 is applied in a slightly different manner. Maintaining attached flow throughout the inlet, i.e. to the diffuser exit, is considered to be the design requirement. Therefore, the surface velocities are nondimensionalized by the diffuser exit surface velocity. Then, if the ratio of maximum velocity to diffuser exit velocity (i.e. the diffusion ratio) exceeds a certain value separation is indicated.

Even though engine inlets proposed for VTOL applications operate at subsonic throat Mach numbers, the Mach number on the inlet internal surface may become locally supersonic and reach Mach numbers as high as 2.0. Based on STOL experimental data, Ref. 1 suggests that these supersonic conditions strongly influence the boundary-layer separation process through shock/boundary-layer interaction. Thus another parameter, peak Mach number, should be useful for predicting boundary-layer separation. The two parameters, diffusion ratio and peak Mach number, will be used throughout this paper as the separation parameters for inlet analysis.

Theoretical boundary-layer calculations could be made to determine the values of diffusion ratio and peak Mach number at which the flow separates for various inlet geometries and flow conditions. However, experimental data from which the limiting values of the separation parameters could readily be determined were available for several STOL inlets (from the tests reported in Ref. 2). Therefore, to test the usefulness of the concept it was decided to use the available experimental data rather than perform the large number of boundary-layer calculations required for a complete theoretical study.

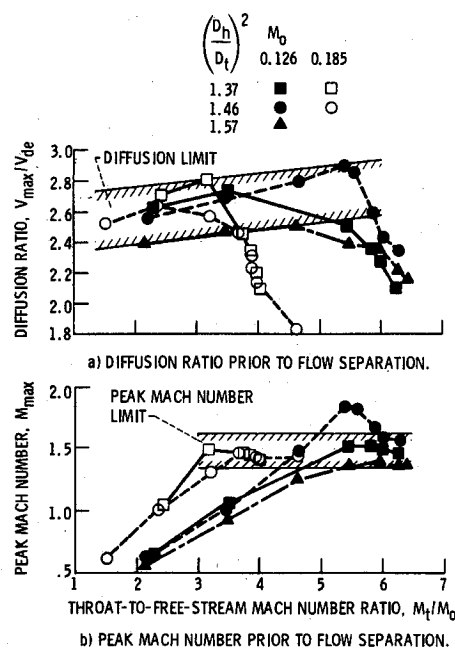


Fig. 2 Experimental separation data for STOL inlets.

The three experimental STOL inlet geometries<sup>2</sup> selected for this study are shown in Fig. 1. These geometries have a  $D_h/D_{max}$  of 0.905 and internal lip contraction ratios,  $(D_h/D_t)^2$ , of 1.37, 1.46, and 1.56.

The experimental flow-separation data for these inlets are illustrated in Fig. 2. These data were obtained by setting the freestream Mach and the throat Mach number (inlet mass flow) and then increasing the inlet incidence angle to the point of observed lip separation. The values of diffusion ratio and peak Mach number plotted in Fig. 2 are obtained at the incidence angle immediately before the flow separates. These angles (not indicated in the figure) depend upon the flow conditions and may differ from point to point.

Figure 2a shows that as throat Mach number (consequently  $M_t/M_0$  for fixed  $M_0$ ) is decreased from its maximum value for each curve the diffusion ratio increases up to a point and then decreases slightly at the lower throat Mach numbers. Thus there appears to be an upper limit on diffusion ratio above which the flow separates at the lower throat Mach numbers. This limit is a weak function of throat Mach number and also a function of contraction ratio but generally lies in the range of 2.4 to 2.9 for these inlets. This range in diffusion ratio limit is indicated as a band in Fig. 2a. If the diffusion ratio limit for any inlet lies below the upper limit range at the high throat Mach numbers, these points will be shown to be peak Mach number limited.

Figure 2b shows that as throat Mach number (consequently  $M_t/M_0$  for fixed  $M_0$ ) is increased from its minimum value for each curve, the peak Mach number increases up to a point and remains relatively constant for the larger throat Mach numbers. Thus there appears to be an upper limit on the peak Mach number above which the flow separates at the higher throat Mach numbers. This limit appears to be a weak function of contraction ratio for the low freestream Mach number but generally lies in the range of 1.4 to 1.6 for these inlets. The range in peak Mach number limit is indicated as a band in Fig. 2b.

In summary, at lower throat Mach numbers the separation-free flow appears to be diffusion ratio limited and at higher throat Mach numbers the separation-free flow appears to be peak Mach number limited.

### Analysis

The experimental results of the previous section will be used to evaluate engine inlets designed for tilt-nacelle VTOL

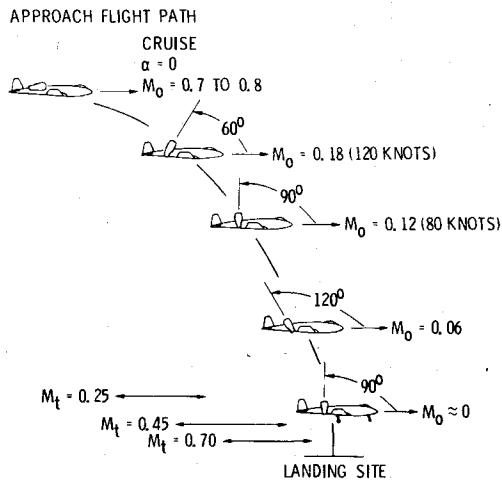


Fig. 3 Representative VTOL flight conditions.

Table 1 Fixed VTOL inlet geometric parameters

<b>Diffuser</b>	
Diameter of exit, $D_e$ , cm	30.48
Ratio of length to exit diameter, $L_d/D_e$	0.55
Ratio of exit flow area to throat area, $A_e/A_t$	1.066
Ratio of disk exit area to throat area, $A_{e,disk}/A_t$	1.269
Location of inflection point, percent of length	50
Maximum local wall angles, deg	8.7
Equivalent conical half-angle, deg	1.5
Contour of inlet	cubic
<b>Centerbody</b>	
Ratio of hub to tip diameters, $D_c/D_e$	0.4
Ratio of major to minor axis	2.0
Contour	ellipse

aircraft. Based on probable flight paths for a tilt-nacelle VTOL aircraft as shown in Fig. 3 the following limited number of flow conditions were selected for analysis: incidence angles up to 90 deg for a freestream Mach number of 0.12 and throat Mach numbers ranging from 0.25 to 0.70.

#### Geometry

The nomenclature used and the principal inlet geometric variables are illustrated in Fig. 1. For the inlets investigated the internal lip geometry and external forebody geometry were varied; however, the diffuser geometry and the centerbody were fixed (Table 1). The internal lip profile was a 2 to 1 ellipse and was characterized by the inlet contraction ratio,  $(D_h/D_t)^2$ , which ranged from 1.46 to 2.8 as shown in Fig. 4. For all the inlets the external forebody profile was a bisuperellipse curve of the form <sup>7</sup>

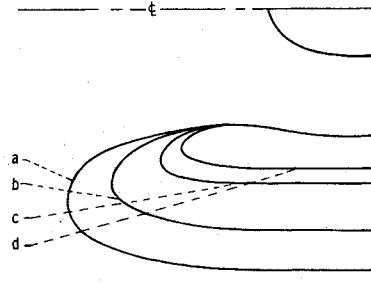
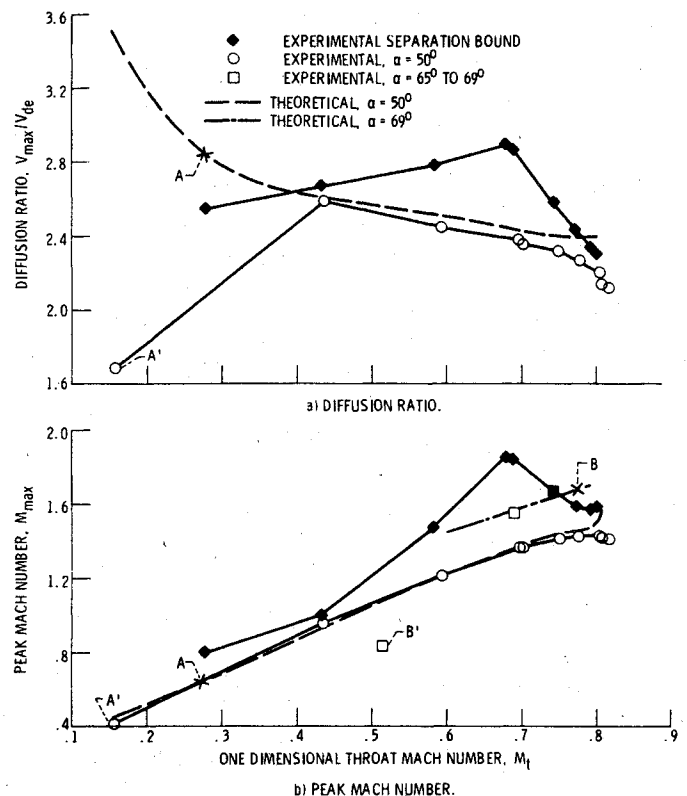
$$(x/\bar{x})^{1.77} + (y/\bar{y})^{2.25} = 1$$

and the design drag divergence Mach number was 0.77. The variables of this equation are indicated in Fig. 1c. However, the external forebody geometric parameters (the ratio of external forebody length to maximum diameter,  $\bar{x}/D_{max}$ , and the ratio of highlight to maximum diameter,  $D_h/D_{max}$ ) varied with contraction ratio (Fig. 4) for the fixed drag divergence Mach number.

#### Method of Solution

The theoretical potential flow at the various operating conditions for the inlets was obtained using the calculation procedures for engine inlets as presented in Ref. 9. Briefly, the basic elements of the potential flow computer program system are: 1) a program for geometry definition, 2) an incompressible potential flow calculation program, and 3) a program to combine basic potential flow solutions into solutions of interest (having specified values of freestream

INLET	$(D_h/D_t)^2$	$(D_h/D_{max})$	$\bar{x}/D_{max}$	$L/D_e$
a	2.8	0.757	0.405	1.148
b	2.2	.802	.345	.979
c	1.65	.874	.290	.803
d	1.46	.905	.193	.735

Fig. 4 Effect of contraction ratio  $(D_h/D_t)^2$  on VTOL tilt-nacelle geometry.Fig. 5 Comparison of theoretical and experimental diffusion ratio and peak Mach number for 1.46 contraction ratio STOL inlet and  $M_o = 0.126$ .

velocity, incidence angle, and inlet mass flow) and also to correct the results for compressibility effects and local supersonic Mach number effects.

The potential flow calculations were used to obtain surface pressure distributions, peak Mach numbers, and diffusion ratios for the several inlet geometries and various flow conditions. All potential flow results shown are for the windward (see Fig. 1) side of the inlet since the most severe flow conditions occur at this position.

#### Results and Discussion

First will be presented a comparison of theoretical and experimental diffusion ratio and peak Mach numbers for the 1.46 contraction ratio STOL inlet of Fig. 1. Then theoretical pressure distributions for the VTOL tilt-nacelle inlets of Fig. 4 will be considered. Finally the theoretical diffusion ratios and

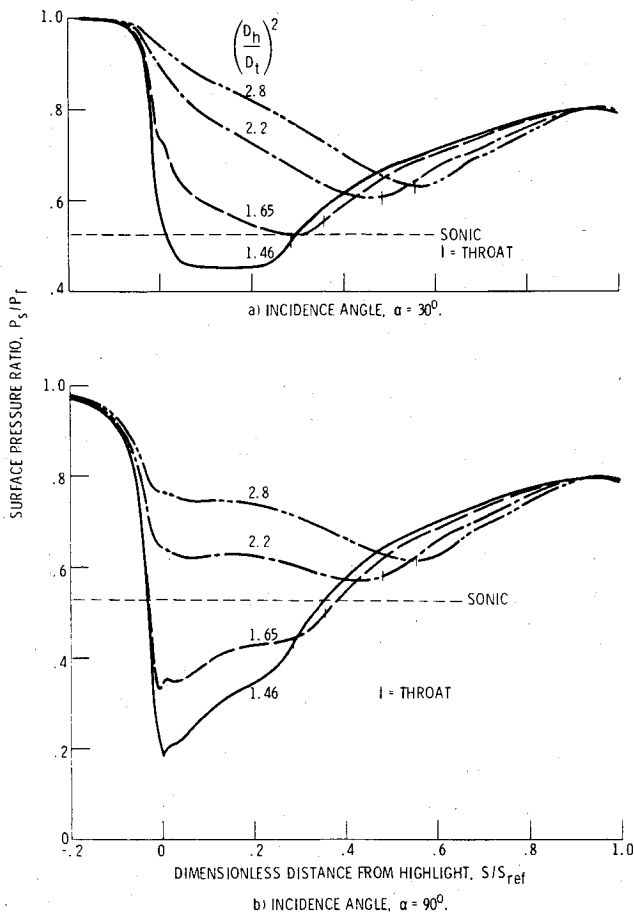


Fig. 6 Theoretical surface pressure ratio distributions for several contraction ratios at  $M_t = 0.7$  and  $M_o = 0.12$ .

Mach numbers for the tilt-nacelle inlets will be presented and evaluated by the experimental separation bounds of the STOL test inlets.

#### Comparison of Theory and Experiment

Figure 5 shows a comparison of the theoretical and experimental diffusion ratio and peak Mach number for a freestream Mach number of 0.126 for the 1.46 contraction-ratio test inlet. Also shown is the experimental separation bound (solid symbols) for this inlet at  $M_o = 0.126$ . Consider the experimental diffusion ratio data for an incidence angle of 50 deg (circular symbols, Fig. 5a). The falloff in the experimental diffusion ratio for  $M_t > 0.75$  is caused by a separation bubble on the inlet lip. As the throat Mach number is decreased, the diffusion ratio tends to increase until the separation limit is reached ( $M_t = 0.4$ ). If the throat Mach number is further reduced say to 0.3 (the experimentally set value) the potential flow theory indicates that the diffusion ratio increases to a value which would lie in the separated flow region above the limit line (point A in Fig. 5a). However, since this point is above the limit, the flow separates and the weight flow drops causing both the throat Mach number and the diffusion ratio to drop as indicated by the experimental data point A' in Fig. 5a. This dropping of weight flow is observed experimentally at all separation conditions.

Figure 5b shows theoretical and experimental peak Mach number curves for two incidence angles 50 and 69 deg. The 50 deg data are shown for comparison with Fig. 5a; note that point A in Fig. 5b is below the peak Mach number limit and separation is therefore not indicated by this parameter. However, as has been already shown, point A in Fig. 5a indicates diffusion-limited separation. This illustrates the conjecture that diffusion, and not peak Mach number, is the limiting parameter at low throat Mach numbers. Next con-

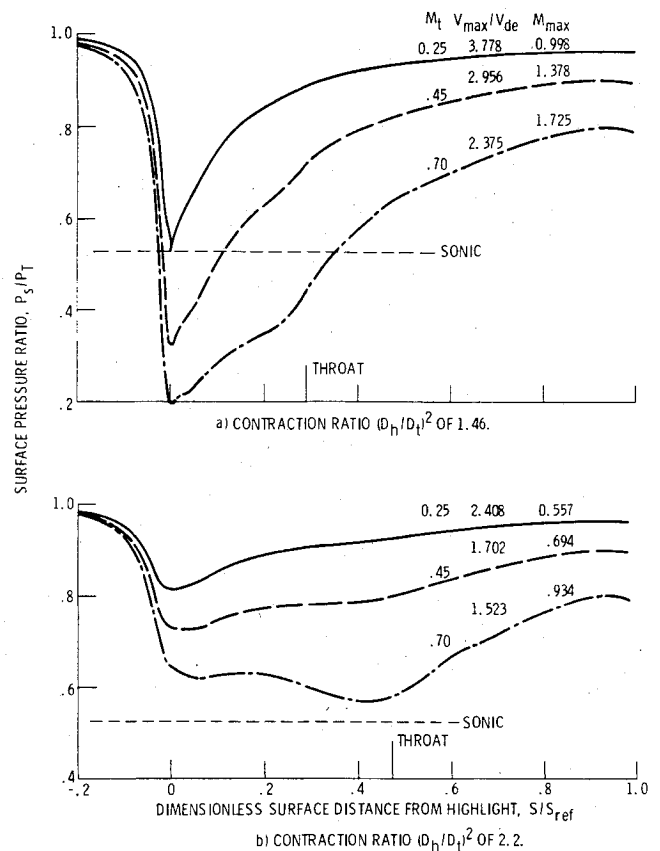


Fig. 7 Theoretical surface pressure distributions for several throat Mach numbers. Incidence angle  $\alpha = 90$  deg and  $M_o = 0.12$ .

sider the higher Mach number region of the 50 deg curves; as throat Mach number is increased the peak Mach number increases as would be expected. The slight falloff in the experimental  $M_{max}$  for  $M_t > 0.75$  is caused by a separation bubble on the inlet lip. However  $M_{max}$  nowhere exceeds the limiting curves and no extensive separation is indicated. To illustrate peak Mach number type separation, theoretical and experimental curves for an incidence angle of 69 deg are shown. As  $M_t$  is increased,  $M_{max}$  increases until the separation limit is reached. If  $M_t$  is further increased to 0.775 (point B on the theory curve) the limit is exceeded and separation is indicated. Therefore, in the experiment the weight flow drops causing both  $M_t$  and  $M_{max}$  to drop as indicated by point B' in Fig. 5b.

#### Sample Theoretical Pressure Distributions

Figure 6 shows the surface pressure ratio as a function of dimensionless distance from highlight for several contraction ratios (Fig. 4), incidence angles of 30 and 90 deg,  $M_t$  of 0.7, and  $M_o$  of 0.12. In general, the surface static pressure ratio increases with increasing contraction ratio and decreases with increasing incidence angle. For incidence angles less than 30 deg (the 30 deg curves are shown in Fig. 6a) little or no diffusion takes place on the inlet lip. At large incidence angles such as 90 deg (Fig. 6b) the curves for contraction ratios of 2.8 and 2.2 still show little or no diffusion on the inlet lip; however, the curves for contraction ratios of 1.65 and 1.46 begin to show significant diffusion on the lip.

A range of operating conditions expected to be particularly severe for a tilt-nacelle inlet is that of a freestream Mach number of 0.12, an incidence angle of 90 deg, and throat Mach number ranging from 0.25 to 0.70 (Fig. 3). These are the conditions for which theoretical results are obtained to illustrate the use of experimental separation limits in inlet design.

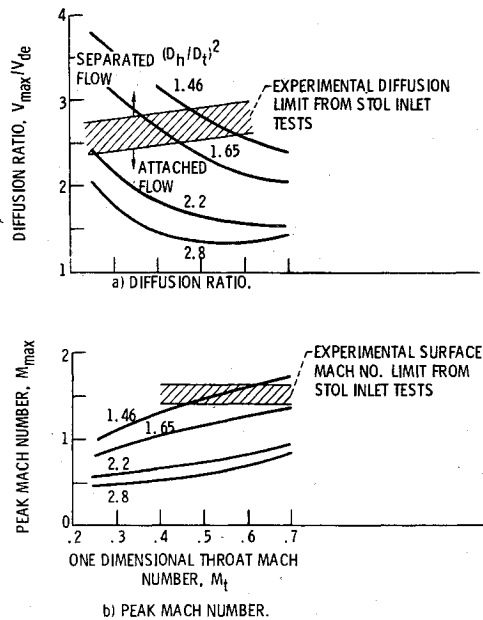


Fig. 8 Theoretical VTOL separation parameters with experimental STOL separation limits vs throat Mach number for  $\alpha = 90^\circ$  deg and  $M_0 = 0.12$ .

First some illustrative pressure distributions are shown in Fig. 7 for tilt-nacelle inlet contraction ratios of 1.46 and 2.2. This figure indicates that the flow becomes locally supersonic for all flow conditions for the 1.46 contraction ratio but remains subsonic for the 2.2 contraction ratio. Figure 7 also shows that decreasing the throat Mach number increases the initial diffusion rate (pressure gradient after minimum pressure point) and the diffusion ratio but lowers the peak Mach number for both contraction ratios. Similar pressure distributions were generated for other contraction ratios to obtain the diffusion ratio and peak Mach number to be presented in the next section.

#### Application of Experimental Separation Bounds to Theoretical Diffusion Ratio and Peak Mach Number

The effects of varying throat Mach number on the parameters diffusion ratio,  $V_{\max}/V_{de}$ , and peak Mach number,  $M_{\max}$ , are shown in Fig. 8 for a freestream Mach number of 0.12 and an incidence angle of  $90^\circ$ . Decreasing the throat Mach number tends to increase  $V_{\max}/V_{de}$  (Fig. 8a) for all contraction ratios; however, increasing the throat Mach number tends to increase the peak Mach number (Fig. 8b). The effect of increasing the contraction ratio is to decrease both parameters  $V_{\max}/V_{de}$  and  $M_{\max}$  at a given throat Mach number.

Figure 8 also shows the experimental separation limits of Fig. 2 superimposed on the potential flow results for the diffusion ratio and peak Mach number. Regions of expected separated and attached flow are shown.

In Fig. 8a, it can be seen that low-throat-Mach-number conditions are likely to lie in the diffusion-limited separation region. This figure also shows that, at a given flow condition, increasing the contraction ratio results in a reduced diffusion ratio. For sufficiently large contraction ratios the diffusion ratio will be in the attached flow region.

In Fig. 8b, it can be seen that increasing the throat Mach number may result in peak Mach numbers which lie in the Mach number-limited separated flow region. For given flow conditions, increasing the contraction ratio a sufficient amount moves the peak Mach number into the attached region.

Figure 8 indicates whether the inlet will separate at  $M_0 = 0.12$  and  $\alpha = 90^\circ$  deg over the range of  $M_t$  indicated. If any other operating conditions (Fig. 3) can produce

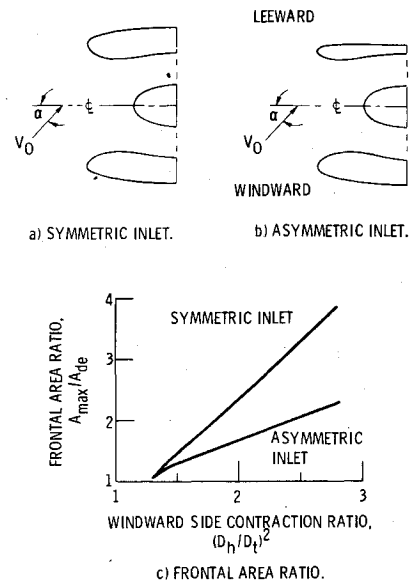


Fig. 9 Comparison of symmetric and asymmetric inlet geometries.

significant separation, then they should be similarly investigated.

This procedure of applying experimental separation limits to theoretical separation parameters permits a coarse screening of inlet designs. To avoid an overly conservative inlet, the contraction ratio could be varied more finely near the separation limit and a more optimum inlet design could be determined by using boundary-layer calculations.

#### Summary of Results

The effect of inlet lip contraction ratio on the aerodynamic performance was investigated for inlets of tilt-nacelle VTOL aircraft. Some specific results of this study are as follows:

- 1) Review of experimental results indicates that two separation parameters are important. These are the diffusion ratio (ratio of maximum surface velocity to diffuser exit velocity) and the peak Mach number (maximum surface Mach number).
- 2) The diffusion ratio is the governing separation parameter at low throat Mach numbers.
- 3) The peak Mach number is the governing separation parameter at high-throat Mach numbers.
- 4) For given flow conditions, increasing the contraction ratio a sufficient amount results in diffusion ratios and peak Mach numbers which are less than the separation-limited values.

#### Concluding Remarks

It should be noted that at larger contraction ratios the designer is faced with larger nacelle maximum diameters (Fig. 4) which result in larger nacelle drag and weight. The optimum design for the tilt-nacelle may be an asymmetric inlet having a large contraction-ratio lip on the windward side where the most severe flow conditions exist and a smaller contraction-ratio lip on the leeward side where less severe flow conditions exist. The ideal design would be a distribution of contraction ratio around the inlet which results in improved low-speed aerodynamic performance and minimum nacelle drag and weight. An example of this approach is shown in Fig. 9.

#### References

- <sup>1</sup>Jakubowski, A.K. and Luidens, R.W., "Internal Cowl Separation at High Incidence Angles," AIAA Paper 75-64, Pasadena, Calif., 1975.
- <sup>2</sup>Miller, B.A., Dastoli, B.J., and Wesoky, H.L., "Effect of Entry-Lip Design on Aerodynamics and Acoustics of High-Throat-Mach-

Number Inlets for the Quiet, Clean, Short-Haul Experimental Engine," NASA TM X-3222, 1975.

<sup>3</sup>Albers, J.A., "Theoretical and Experiment Internal Flow Characteristics of a 13.97-Centimeter-Diameter Inlet at STOL Takeoff and Approach Conditions," NASA TN D7185, 1973.

<sup>4</sup>Felderman, E.J. and Albers, J.A., "Comparison of Experimental and Theoretical Boundary-Layer Separation for Inlets at Incidence Angle at Low-Speed Conditions," NASA TM X-3194, 1975.

<sup>5</sup>Albers, J.A. and Miller, B.A., "Effect of Subsonic Inlet Lip Geometry on Predicted Surface and Flow Mach Number Distributions," NASA TN D-7446, 1973.

<sup>6</sup>Albers, J.A. and Felderman, E.J., "Boundary-Layer Analysis of Subsonic Inlet Diffuser Geometries for Engines Nacelles," NASA TN D-7520, 1974.

<sup>7</sup>Albers, J.A., Stockman, N.O., and Hirn, J.J., "Aerodynamic Analysis of Several High Throat Mach Number Inlets for the Quiet Clean Short-Haul Experimental Engine," NASA TM X-3183, 1975.

<sup>8</sup>Smith, A.M.O., "High-Lift Aerodynamics," *Journal of Aircraft*, Vol. 12, June 1975, pp. 501-530.

<sup>9</sup>Stockman, N.O., "Potential and Viscous Flow in VTOL, STOL or CTOL Propulsion System Inlets," AIAA Paper 75-1186, Anaheim, Calif., 1975.

*From the AIAA Progress in Astronautics and Aeronautics Series..*

## AERODYNAMIC HEATING AND THERMAL PROTECTION SYSTEMS—v. 59 HEAT TRANSFER AND THERMAL CONTROL SYSTEMS—v. 60

*Edited by Leroy S. Fletcher, University of Virginia*

The science and technology of heat transfer constitute an established and well-formed discipline. Although one would expect relatively little change in the heat transfer field in view of its apparent maturity, it so happens that new developments are taking place rapidly in certain branches of heat transfer as a result of the demands of rocket and spacecraft design. The established "textbook" theories of radiation, convection, and conduction simply do not encompass the understanding required to deal with the advanced problems raised by rocket and spacecraft conditions. Moreover, research engineers concerned with such problems have discovered that it is necessary to clarify some fundamental processes in the physics of matter and radiation before acceptable technological solutions can be produced. As a result, these advanced topics in heat transfer have been given a new name in order to characterize both the fundamental science involved and the quantitative nature of the investigation. The name is Thermophysics. Any heat transfer engineer who wishes to be able to cope with advanced problems in heat transfer, in radiation, in convection, or in conduction, whether for spacecraft design or for any other technical purpose, must acquire some knowledge of this new field.

Volume 59 and Volume 60 of the Series offer a coordinated series of original papers representing some of the latest developments in the field. In Volume 59, the topics covered are 1) The Aerothermal Environment, particularly aerodynamic heating combined with radiation exchange and chemical reaction; 2) Plume Radiation, with special reference to the emissions characteristic of the jet components; and 3) Thermal Protection Systems, especially for intense heating conditions. Volume 60 is concerned with: 1) Heat Pipes, a widely used but rather intricate means for internal temperature control; 2) Heat Transfer, especially in complex situations; and 3) Thermal Control Systems, a description of sophisticated systems designed to control the flow of heat within a vehicle so as to maintain a specified temperature environment.

*Volume 59—432 pp., 6 × 9, illus. \$20.00 Mem. \$35.00 List*

*Volume 60—398 pp., 6 × 9, illus. \$20.00 Mem. \$35.00 List*

TO ORDER WRITE: Publications Dept., AIAA, 1290 Avenue of the Americas, New York, N.Y. 10019